

Size effects on the structure and phase transition behavior of baddeleyite TiO_2

Varghese Swamy^{a,*}, Leonid S. Dubrovinsky^b, Natalia A. Dubrovinskaia^b,
Falko Langenhorst^b, Alexandre S. Simionovici^c, Michael Drakopoulos^c,
Vladimir Dmitriev^d, Hans-Peter Weber^d

^a*School of Physics and Materials Engineering, Monash University, Clayton Campus, P.O. Box 69M, Victoria 3800, Australia*

^b*Bayerisches Geoinstitut, Universität Bayreuth, Bayreuth D-95440, Germany*

^c*European Synchrotron Radiation Facility, Grenoble 38043, France*

^d*SNBL, European Synchrotron Radiation Facility, Grenoble 38043, France*

Received 31 January 2005; accepted 24 February 2005 by A.K. Sood

Available online 11 March 2005

Abstract

High-pressure structural transitions in nanocrystalline systems are of significant interest as models of first-order phase transitions. We demonstrate size-induced lattice expansion and significant atomic rearrangements in the crystal structure of nanocrystalline high-pressure baddeleyite- TiO_2 . The α - PbO_2 structured TiO_2 recovered after dozens of pressure cycles in the α - PbO_2 -baddeleyite pressure field displayed elongate 25–35 nm crystallites, compared to starting 34-nm anatase crystallites, suggesting crystallite coherency across anatase, baddeleyite, and α - PbO_2 structures and ‘single structural domain’ behavior of the nanocrystalline system.

© 2005 Elsevier Ltd. All rights reserved.

PACS: 61.46.+w; 61.50.Ks; 64.70.Nd; 64.30.t

Keywords: A. Nanostructured materials; D. High-pressure; D. Phase transition

1. Introduction

Pressure-induced structural phase transitions in nanocrystalline materials attract significant attention as models to understand the kinetics and microscopic mechanisms of first-order solid-solid phase transitions [1,2]. They also draw attention because of the possible role of nanocrystalline phases within planetary interiors [3] and because of the potential use of dense nanometer-sized phases in shocked

earth’s crystal materials and in meteorites and possibly around presolar stars to constraining their conditions of formation and evolution [4–6]. Several high-pressure studies on nanocrystalline semiconductor systems such as CdSe and CdS have shown that these nanocrystals behave as nearly defect-free single structural domains that cycle through the transitions between four-coordinate and six-coordinate structures reproducibly, with attendant simple phase transition kinetics [7–9]. While considerable understanding of the microscopic mechanisms of pressure-induced first-order solid-solid phase transition has been achieved by investigating CdSe type nanocrystals, the size effects on the detailed atomic arrangements in the crystal structures and on other physical properties of the resulting high-pressure phases

* Corresponding author. Tel.: +61 3 9905 5323; fax: +61 3 9905 4940.

E-mail address: varghese.swamy@spme.monash.edu.au (V. Swamy).

have not been investigated in detail. As the crystallite size shrinks to the nanoscale dimensions (up to few hundred nanometers), a significant fraction of the constituent atoms of a material is at or near the surface in coordination environments that could be substantially different from those in the bulk. Such changes in the atomic arrangements may not be clearly noticed in high symmetry systems such as Cd chalcogenides. We, therefore, chose to study nanocrystalline TiO₂ to understand the size-effects on the crystal structure, bulk modulus, and crystallite size evolution across the pressure-induced orthorhombic (*Pbcn*) α -PbO₂-monoclinic (*P2₁/c*) baddeleyite structural phase transition.

TiO₂ is a particularly important model system in the study of phase transition behavior of oxides. First, bulk (microparticle) TiO₂ has long served mineral physicists as a model system in the study of the pressure-induced phase transitions of rutile-structured stishovite SiO₂ in the earth's mantle [10]. Secondly, nanocrystalline TiO₂ has been used as a prototype to investigate the size-dependent phase transition behavior of nanoscale oxides in terrestrial environments [3]. Furthermore, in our view, the low-symmetry baddeleyite TiO₂ is an ideal case for examining size-induced changes in the crystal structure because of the extra degrees of freedom in the fractional atomic coordinates.

In bulk TiO₂, the α -PbO₂ phase forms from anatase, rutile, or brookite at 2.5–12 GPa [11–15]. Beyond about 12 GPa, TiO₂ adopts the baddeleyite structure that upon decompression converts back to α -PbO₂ at about 7 GPa [16–18]. Titanium is six-coordinated to oxygen in all the lower pressure structures, including α -PbO₂, whereas in the baddeleyite structure it is seven-coordinated. The pressure-induced phase transitions of nanocrystalline TiO₂, however, are not well established. α -PbO₂ was reported to form at 4.75 GPa and 250 °C from a 38 nm-sized anatase–rutile mixture [19]. 7–11 nm anatase was observed to persist, using Raman scattering data obtained in a diamond anvil cell (DAC), to 24 GPa at room temperature before turning amorphous [20]. Room-temperature DAC X-ray diffraction (XRD) data were used to suggest that 30 nm rutile in a rutile–anatase mixture transformed directly to baddeleyite at 8.7 GPa while the anatase persisted to 16.4 GPa where it amorphized [21]. Pressure-induced amorphization was not observed at room temperature for a 34 nm anatase in our DAC XRD study [22]. Instead, direct transformation to baddeleyite was observed at 18 GPa. In contrast to the enhanced pressure stability of nanocrystalline anatase, the pressure stability of nanocrystalline rutile decreases with decreasing crystallite size [6,14].

2. Experimental details

The nanocrystalline TiO₂ used as starting material in our experiments was obtained from a commercial supplier [32]. It consists of phase-pure (>99.5%) equiaxial anatase

crystallites with an average diameter of 34 nm (as determined by the supplier using the Scherrer, BET, and TEM methods). Although majority of the crystallites fall near 34 nm, we estimated a narrow crystallite size distribution in the range of 30–40 nm from TEM data and an average size of 32(5) nm based on Williamson–Hall plot [26] of powder XRD data.

Nanocrystalline α -PbO₂ and baddeleyite structured TiO₂ were synthesized in electrically- and laser-heated diamond anvil cells (DACs) as described earlier [23]. We mounted diamonds with culets of 250 or 300 μ m on the seats with 30° opening allowing us to collect diffraction data to 0.9 Å in 4-pin DACs. Gaskets were made of a 250 μ m thick Re sheet that was pre-indented to 30–33 μ m thickness. Holes of 80–100 μ m diameter were drilled in the gasket, centered on the indentation. The sample was packed into the hole and the gasket compressed between the opposing diamonds. To synthesize the nanocrystalline and bulk baddeleyite phases, we compressed the appropriate starting material in a DAC gradually to about 37 GPa, then heated the sample in electrically- or laser-heated DACs between 850 and 900 K for 4–5 h, and subsequently cooled to room temperature. This produced good quality baddeleyite TiO₂ and also relieved the deviatoric stress in the samples, as judged from the XRD spectra.

The pressure-induced changes in the nanocrystals were monitored principally with angle-dispersive powder XRD at the BM01 and ID22 beamlines of the European Synchrotron Radiation Facility (ESRF), Grenoble, France. At the BM01 beamline of ESRF, the data were obtained with the MAR345 detector using an X-ray beam of wavelength 0.6996 Å and size of 20×20 μ m, and at ID22, we used a CCD area detector and a highly focused beam of 0.62 Å wavelength and 2×5 μ m size. The detector-to-sample distance varied in different experiments from 60 to 350 mm. The diffraction images obtained were integrated using the FIT2D program [33] to convert them to conventional diffraction spectra. Full-profile refinements of the XRD data were carried out using the GSAS package [34]. We used a 5 μ m thick Au (99.99%) wire, placed near the center of the pressure chamber, as the internal pressure standard. At 35 GPa, the pressure variation in the center of the sample (within the size of the X-ray beam) was less than 1 GPa.

We carried out additional DAC XRD experiments, including those on the bulk phases, at the Bayerisches Geoinstitut (BGI), Universität Bayreuth, Germany. Although in some of the DAC experiments Ar, NaCl, or CsCl was used as a pressure-transmitting medium, we did not observe significant differences in the results between experiments with and without the pressure medium, probably because heating relaxed stresses in the DACs.

In order to examine possible size effects on the vibrational spectra of the high-pressure TiO₂ polymorphs, we collected room-temperature, high-pressure Raman scattering data from samples in the DACs using a LabRam

spectrometer at the BGI equipped with a He–Ne laser operating at 632 nm. The crystallite sizes were obtained with low-resolution transmission electron microscopy (TEM) at the Bayerisches Geoinstitut (BGI). The chemical composition of the samples was verified using a LEO-1530 scanning electron microscope and a PHILIPS CM20 FEG analytical transmission electron microscope (ATEM) operating at 200 kV at BGI, and we found that high pressure/temperature treatment did not result in any chemical reactions.

3. Results and discussion

We investigated pressure-induced changes in nanocrystalline TiO_2 in compression-decompression cycles spanning 0–46 GPa. A comparison of the in situ high-pressure XRD spectra of the nanocrystalline and bulk baddeleyite structures at 34(1) GPa shown in Fig. 1 reveals distinct differences at medium to high 2θ ranges. Additional diffraction peaks are seen in the case of nanocrystalline baddeleyite. Rietveld refinement of the data in the space

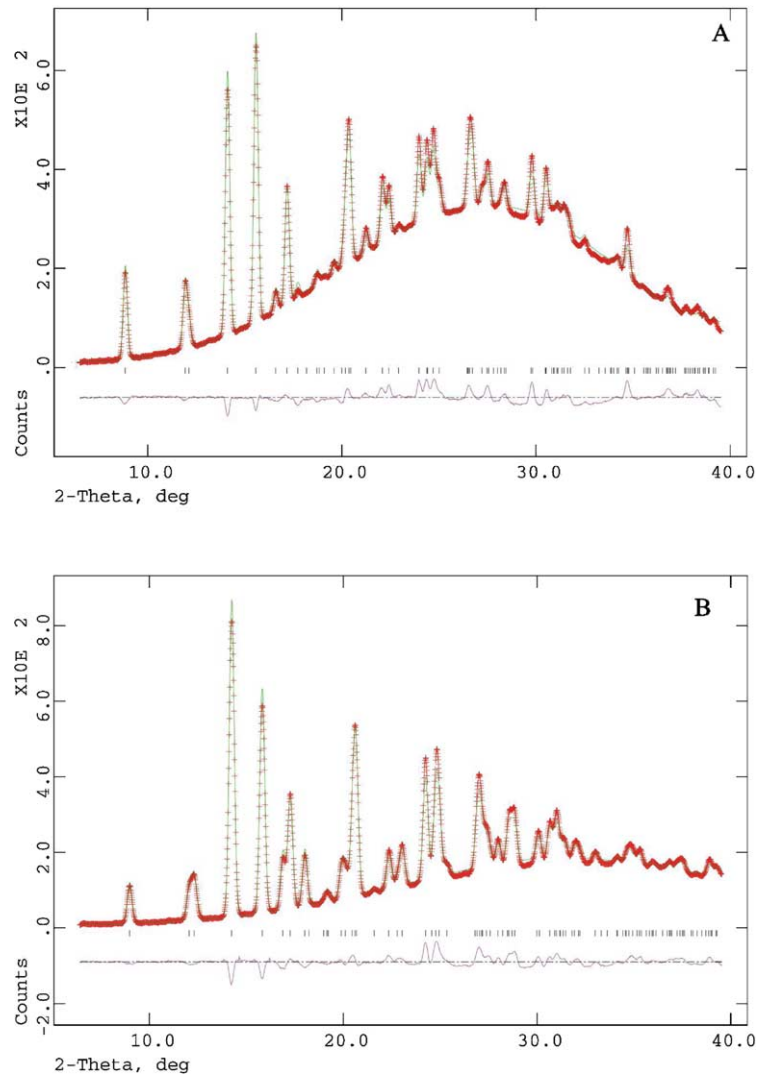


Fig. 1. Powder XRD spectra of baddeleyite structured TiO_2 recorded at room temperature and 34(1) GPa along with calculated and difference (experimental-calculated) XRD profiles obtained from Rietveld analyses. The short vertical bars indicate XRD peak positions obtained in the Rietveld refinement. (A) The baddeleyite synthesized from nanocrystalline anatase has the following crystal structural data: $a=4.589(1)$ Å, $b=4.849(1)$ Å, $c=4.736(1)$ Å, and $\beta=98.6(1)^\circ$. Space group $P2_1/c$. The x , y , and z fractional atomic coordinates for the titanium and two oxygen atoms in the asymmetric unit are: Ti = 0.309(1), 0.045(2), 0.218(1); O₍₁₎ = 0.056(1), 0.347(1), 0.282(1); and O₍₂₎ = 0.425(1), 0.727(1), 0.463(1). $R_p=4.6\%$ and $R_{wp}=5.4\%$. (B) The baddeleyite synthesized from microcrystalline anatase has the following crystal structural data: $a=4.525(1)$ Å, $b=4.767(1)$ Å, $c=4.718(1)$ Å, and $\beta=98.7(1)^\circ$. The fractional atomic coordinates for titanium and oxygen atoms are: Ti = 0.276(2), 0.037(1), 0.212(2); O₍₁₎ = 0.109(1), 0.382(1), 0.261(1); and O₍₂₎ = 0.435(1), 0.768(1), 0.488(1). $R_p=3.0\%$ and $R_{wp}=3.5\%$.

group $P2_1/c$ yielded comparable good quality solutions (Fig. 1). Significantly, the a and b unit cell parameters of the nanocrystalline baddeleyite are 1.4 and 1.7% larger than those of the bulk phase. Similarly, the unit cell constant c is marginally bigger (0.4%), whereas the cell angle β is essentially the same in comparison with the bulk structure parameters. The calculated unit cell volume for the nanocrystalline baddeleyite at 34(1) GPa, 104.20 \AA^3 , is about 3.6% larger than that of the bulk structure, 100.60 \AA^3 , clearly demonstrating size-induced lattice expansion.

Not only does size influence the lattice parameters of baddeleyite TiO_2 , the atomic arrangement in the structure also changes significantly at the nanoscale (compare the fractional atomic coordinates listed in Fig. 1 for the two structures). This can be clearly appreciated by comparing the Ti–O and O–O distances in the two structures. In the bulk baddeleyite, the calculated Ti–O distances at 34(1) GPa and room temperature are (in \AA): 1.839, 1.891, 1.914, 1.995, 2.005, 2.046, and 2.187. The O–O distances vary from 2.430 to 3.378 \AA (12 atoms). The corresponding Ti–O distances in the nanocrystalline baddeleyite are (in \AA): 1.920, 1.955, 1.931, 1.821, 2.278, 1.917, and 2.108, with the O–O distances varying from 2.405 to 3.188 \AA . Thus, up to 13.6% change in the Ti–O distances, with respect to the bulk structure, is seen in the nanocrystalline structure. This represents a severe distortion of the atomic arrangement at the nanoscale in relation to the extended structure.

The size-induced distortion of the atomic arrangement in the crystal structure leads to modification of the lattice vibrational characteristics of baddeleyite, as revealed in the Raman spectra. Although details of the size effect on Raman scattering are important, we use Raman data here only to illustrate the modification of vibrational spectra originating purely from size reduction. In Fig. 2 Raman spectra obtained from bulk and nanocrystalline baddeleyite TiO_2 at 34(1) GPa are presented. The most noticeable changes

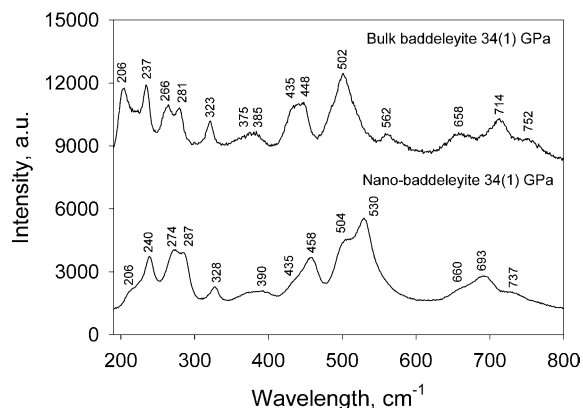


Fig. 2. Raman spectra of baddeleyite structured TiO_2 recorded at room temperature and 34(1) GPa. *Top*: Raman spectrum of bulk baddeleyite. *Bottom*: Raman spectrum of nanocrystalline baddeleyite. The features of the two spectra are discussed in the text.

seen in the spectrum of the nanocrystalline material are: the significant reduction of intensities for the 206, 240, 435, and 658 cm^{-1} bands, the appearance of the peak at 530 cm^{-1} , and the disappearance of the 562 cm^{-1} peak. Most of the Raman bands of the nanocrystalline material are shifted to relatively higher frequencies at this pressure. The frequencies of the bands around 693 and 731 cm^{-1} are, however, systematically lower for the nanophase. Such complex differences in the spectra are not easily explained in terms of the differences in molar volumes and compressibilities through mode Grüneisen parameters, or confinement effects; they have their origins in the local atomic structures of the bulk and nanocrystalline phases and possibly in the mixing of interior lattice and surface vibrational modes. Taken together, our XRD and Raman data suggest that atomic reorganizations in finite sized crystals are not confined to near the surfaces, but extend to the interior of the crystallites.

The room-temperature pressure-volume data obtained on thermally-relaxed and/or Ar loaded nanocrystalline baddeleyite at 15–46 GPa (Fig. 3) can be described by the following Birch equation of state [25]: zero-pressure bulk modulus, $K_{300} = 298(5) \text{ GPa}$; pressure derivative of the bulk modulus, $K' = 3.9(1)$; and zero-pressure volume, $V_0 = 114.61(2) \text{ \AA}^3/\text{unit cell}$. Interestingly, the K_{300} and K' for the nanophase are similar to those of the bulk [14,23,24], but the V_0 differs by about 3.7%. The variation in bulk modulus values between bulk and nanocrystalline phases of anatase [22] and baddeleyite TiO_2 is similar to that seen in some other materials. For example, the bulk and nanocrystalline forms of $\gamma\text{-Fe}_2\text{O}_3$ have different bulk modulus values while

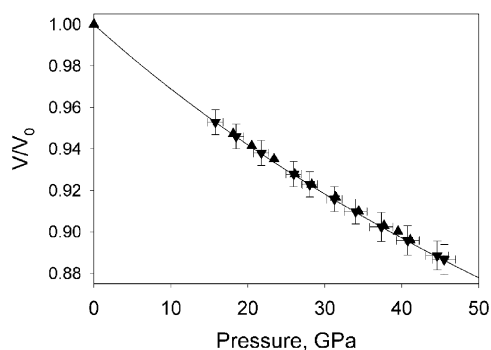


Fig. 3. Room-temperature pressure versus volume data of nanocrystalline (inverted triangles) and macrocrystalline (upright triangles) baddeleyite TiO_2 . The data for the nanocrystalline phase are from this study while those for the macrocrystalline phase from Ref. [24]. The curve represents the pressure–volume relationship for the nanocrystalline baddeleyite calculated using the following Birch–Murnaghan equation parameters [25]: zero-pressure bulk modulus at 300 K, $K_{300} = 298(5) \text{ GPa}$; pressure derivative of the bulk modulus, $K' = 3.9(1)$; and zero-pressure volume, $V_0 = 114.61(2) \text{ \AA}^3/\text{unit cell}$. The equivalent parameters for the macrocrystalline baddeleyite are [24]: $K_{300} = 303(5) \text{ GPa}$, $K' = 3.9(2)$; and $V_0 = 110.48(5) \text{ \AA}^3/\text{unit cell}$.

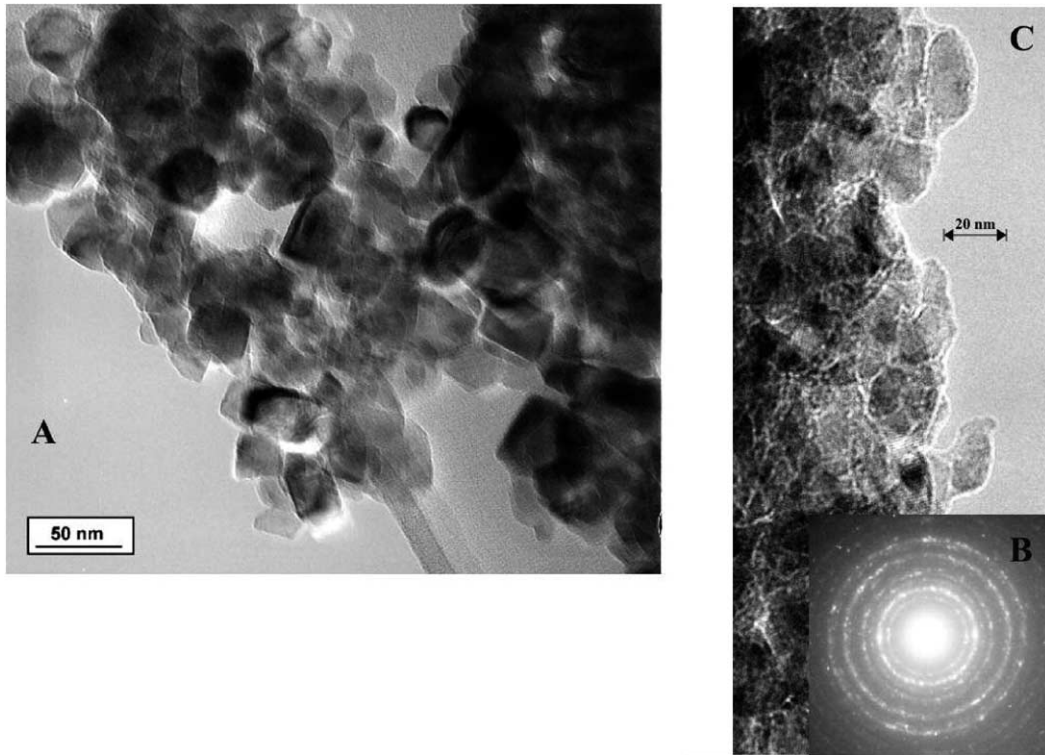


Fig. 4. (A) TEM image of the starting nanocrystalline anatase. The crystallites are equiaxial with an average diameter of 34 nm (size range 30–40 nm). (B) Electron diffraction of the α -PbO₂ structured TiO₂ recovered from the DAC after 50 compression-decompression cycles in the pressure range where bulk α -PbO₂ and baddeleyite structures are stable (up to 40 GPa). (C) TEM image of the recovered α -PbO₂ sample shown in (B). The crystallites are elongate and have sizes in the range of 25–35 nm with an average diameter of about 30 nm.

those of the α -Fe₂O₃ form do not show significant difference in bulk modulus values [35]. More work is needed to understand the size effect on this aspect of high-pressure behavior.

The size and shape changes of the nanocrystals owing to structural transformations were examined by comparative TEM of the starting anatase and samples quenched to room-pressure in the DAC after 50 compression-decompression cycles in the 0–40 GPa pressure range. The baddeleyite structure is not quenchable even as nanocrystals and could not be examined under TEM. As seen in Fig. 4, the starting anatase has fairly equant crystallites with an average size of 34 nm (30–40 nm range). A recovered α -PbO₂ showed mostly elongate crystallites of 25–35 nm (average of 30-nm) (Fig. 4). The size reduction in the α -PbO₂ is approximately consistent with the density difference between the two phases. Crystallite coarsening as result of sintering could not be observed in the transformed material, despite laser- and electrical-heating. This indicates that the majority of the crystallites are preserved as coherent units across multiple transitions involving 6–7 Ti–O coordination change among anatase, α -PbO₂, and baddeleyite. We do not have direct TEM observations on the unrecoverable baddeleyite-TiO₂

nanocrystals. However, using Williamson–Hall plots of XRD data we found that the crystallite sizes in all phases (starting nanocrystalline anatase, baddeleyite, and recovered α -PbO₂) are in the 28–33 nm range within experimental errors. This is suggestive of the ‘single structural domain’ behavior of the nanocrystalline system, as seen for the semiconductors Si and CdSe [2,7,8,27].

The crystallite shape changes accompanying pressure-induced phase transitions have been used as evidence of coherent transformation mechanism in Si and CdSe nanocrystals [2,8,27]. In Si, for example, the diamond-primitive hexagonal structure transition has been documented to be accompanied by shape change. Because the high-pressure phases of Si and CdSe are not recoverable for observation under TEM, these investigations relied on indirect methods, such as X-ray diffraction peak widths [2] or simulation of XRD patterns [8] of the unquenchable high-pressure phases, to arrive at shape changes accompanying structural transitions. The fortuitous preservation of the high-pressure α -PbO₂ crystallites to ambient conditions allows us direct observation under TEM of the crystallite shapes, and the observed elongate shape of this phase in contrast to the equant shape of the starting anatase

crystallites (Fig. 4), again supports the suggestion that low-index equiaxial crystallites are converted to (presumably) high-index high-energy surfaces in the high-pressure phase in consonance with crystallite integrity in the nanocrystals [27,28].

Modifications to materials properties when going from the bulk to nanocrystalline size regimes are well documented [29,30]. As demonstrated by our Rietveld results of nanocrystalline and bulk baddeleyite TiO_2 , for materials with internal degrees of freedom in the structure (which constitute the majority of crystal structures) changes in the atomic arrangements effected by size reduction is a distinct possibility. The use of nanocrystals as models of solid–solid phase transitions (in bulk) assumes that the material retains the bulk structural characteristics at the nanoscale which we demonstrate is not generally true. The structural changes affect the vibrational properties and this, in turn, should affect the thermodynamic stability of the nanophases (A thermodynamic analysis as done for Cd chalcogenides [27, 28,31] cannot be carried out for the nanocrystalline TiO_2 phases now because critical data such as surface energies are missing for the high-pressure phases). Therefore, caution should be exercised when using nanometer-sized inclusion phases as pressure/temperature constraints of formation and evolution of planetary materials [4]. We have observed crystallite coherency involving three phases (that means the original crystallite size is recoverable across pressure-induced phase transitions if not trapped by metastable states) and size-induced crystal structural changes in a nanocrystalline oxide. Such behavior may be prevalent in other classes of nanocrystalline systems also, and can potentially be used for synthesizing structurally-tuned novel nanocrystalline materials.

References

- [1] K. Jacobs, A.P. Alivisatos, *Rev. Mineral. Geochem.* 44 (2001) 59.
- [2] S.H. Tolbert, et al., *Phys. Rev. Lett.* 76 (1996) 4384.
- [3] J.F. Banfield, H. Zhang, *Rev. Mineral. Geochem.* 44 (2001) 1.
- [4] S.L. Hwang, et al., *Science* 288 (2000) 321.
- [5] R. Ash, *Meteor. Planet. Sci.* 36 (2001) 583.
- [6] S.-Y. Chen, P. Shen, *Phys. Rev. Lett.* 89 (2002) 96101.
- [7] C.-C. Chen, et al., *Science* 276 (1997) 398.
- [8] J.N. Wickham, et al., *Phys. Rev. Lett.* 84 (2000) 923.
- [9] K. Jacobs, et al., *Science* 293 (2001) 1803.
- [10] L.-G. Liu, *Science* 199 (1978) 422.
- [11] T. Ohsaka, et al., *Solid State Commun.* 30 (1979) 345.
- [12] K. Lagarec, S. Desgreniers, *Solid State Commun.* 94 (1995) 519.
- [13] P.G. Simons, F. Dacheville, *Acta Crystallogr.* 23 (1967) 334.
- [14] J.S. Olsen, et al., *J. Phys. Chem. Solids* 60 (1999) 229.
- [15] T. Arlt, et al., *Phys. Rev. B* 61 (2000) 14414.
- [16] H. Sato, et al., *Science* 251 (1991) 786.
- [17] J. Tang, S. Endo, *J. Am. Ceram. Soc.* 76 (1993) 796.
- [18] L. Gerward, J.S. Olsen, *J. Appl. Cryst.* 30 (1997) 259.
- [19] S.C. Liao, et al., *Nanostruct. Mater.* 11 (1999) 553.
- [20] Z.W. Wang, S.K. Saxena, *Solid State Commun.* 118 (2001) 75.
- [21] Z.W. Wang, et al., *J. Phys.: Condens. Matter* 13 (2001) 8317.
- [22] V. Swamy, et al., *Solid State Commun.* 125 (2003) 111.
- [23] L.S. Dubrovinsky, et al., *Nature* 410 (2001) 653.
- [24] V. Swamy, et al., *J. Alloys Compd.* 340 (2002) 46.
- [25] O.L. Anderson, *Equations State Solids Geophys. Ceram. Sci.* 1995. p. 405.
- [26] D. Machon, et al., *J. Phys.: Condens. Matter* 15 (2003) 7227.
- [27] S.H. Tolbert, A.P. Alivisatos, *Science* 265 (1994) 373.
- [28] S.H. Tolbert, A.P. Alivisatos, *Ann. Rev. Phys. Chem.* 46 (1995) 595.
- [29] J.F. Banfield, A. Navrotsky (Eds.), *Reviews in Mineralogy Geochemistry* vol. 44 (2001) p. 350.
- [30] G.C. Hadjipanayis, R.W. Siegel (Eds.), *Nanophase Materials: Synthesis–Properties–Applications*, Kluwer Academic Publishers, Dordrecht, 1994.
- [31] M. Haase, A.P. Alivisatos, *J. Phys. Chem.* 96 (1992) 6756.
- [32] <http://www.altairnano.com>.
- [33] A. Hammersley, *Computer program FIT2D* (ESRF, Grenoble), 1998.
- [34] A.C. Larson, R.B. Von Dreele, *Generalized Crystal Structure Analysis System. Report LAUR 86-748*, Los Alamos National Laboratory, NM, USA, 1994.
- [35] J.Z. Jiang, et al., *Europhys. Lett.* 44 (1998) 620.